

Evaluating the Separation of Amphetamines by Electrospray Ionization Ion Mobility Spectrometry/MS and Charge Competition within the ESI Process

Laura M. Matz and Herbert H. Hill, Jr.*

Department of Chemistry, Washington State University, Pullman, Washington 99164-4630

The rapid increase in amphetamine abuse for recreational purposes has created a need for fast analysis and detection methodologies. For the first time, we show the separation of six amphetamines by ESI-IMS/MS. A complete analysis can be performed in 70 s, which is faster than traditional chromatographic techniques. In addition, ESI-IMS/MS was found to provide low detection limits for the six compounds (15.4 ppb for ethylamphetamine). Charge competition between amphetamines was found to occur at high amphetamine concentrations. The degree of preferential ionization was dependent on the functional group placed on the amine. Both one-analyte and two-analyte calibration curves were evaluated on the basis of the ion evaporation model. Evaporation rates were determined for the six amphetamines, and the rates were correlated with the degree of selective ionization. Evaluation of three typical ESI solvent compositions showed that the addition of a modifier (acetic acid and formic acid) enhanced the degree of preferential ionization for some amphetamines and increased the effect of charge competition. The solvent studies show the complexity of ESI and provide possible strategies for altering the amount of charge competition between analytes. Overall, ESI-IMS/MS appears to be a promising technique because of its sensitivity and rapid separation times for the amphetamines in aqueous samples; however, further research employing biological samples is required before it can be recommended as a mainstream technique.

Amphetamines are central nervous system stimulants that produce hallucinogenic and euphoric effects when administered.¹ The rising recreational abuse of amphetamines has increased the need for rapid and sensitive detection systems.² Typically, gas chromatography coupled with MS (GC/MS) is employed for amphetamine analysis (see review in ref 2). Although GC/MS is known to be a sensitive technique for amphetamine analysis, a derivitization step is sometimes required because of similar fragmentation patterns for amphetamines and, consequently, poor diagnostic ions in the mass spectrum². To a lesser extent, liquid

chromatography (LC) with MS detection has been employed for amphetamine analysis,³ although the chromatographic separations have lengthy analysis times, which decreases sample throughput for toxicology laboratories. The separation time in ion mobility spectrometry (IMS) is milliseconds, thus allowing for faster analysis.⁴ The separation of MDMA and MDEA in hair samples by IMS (with a radioactive ionization source) was previously evaluated.⁵ More recently, our lab showed the partial separation of amphetamine and methamphetamine via a high-resolution ESI-IMS/MS system.⁶

Unlike chromatographic methods coupled with MS, the ionization occurs prior to the IMS separation. Any selective ionization within the ionization process will be observed in the measured IMS peak intensities and will influence quantification. Thus, it is important to understand preferential ionization processes and ESI parameters that can reduce or eliminate the degree of selective ionization. The eventual analysis of biological samples should employ an internal standard to account for selective ionization processes that occur as a result of matrix effects.

The introduction of electrospray ionization (ESI) as an ionization process for MS^{7–9} and IMS^{10–13} has enabled the analysis of nonvolatile compounds and liquid-phase ionization. Although the utility of ESI has been realized, the mechanism by which ions are formed is still not completely understood.^{9,14} Two general mechanisms have been proposed: the charge residue model (CRM) (Dole,¹⁵) and the ion evaporation model (IEM) (Iribarne

(3) Maurer, H. J. *Chromatogr. B* **1998**, *713*, 3–25.

(4) Wu, C.; Siems, W. F.; Asbury, G. R.; Hill, H. H., Jr. *Anal. Chem.* **1998**, *70*, 4929–4938.

(5) Keller, T.; Miki, A.; Regenscheit, P.; Dirnhofer, R.; Schneider, A.; Tsuchihashi, H. *Forensic Sci. Int.* **1998**, *94*, 55–63.

(6) Wu, C.; Siems, W. F.; Hill, H. H., Jr. *Anal. Chem.* **2000**, *72*, 396–403.

(7) Yamashita, M.; Fenn, J. B. *J. Phys. Chem.* **1984**, *88*, 4451.

(8) Aleksandrov, M. L.; Gall, L. N.; Drasnov, V. N.; Nikolaev, V. I.; Pavlenko, V. A.; Sukurov, V. A. *Dokl. Akad. Nauk. SSSR* **1984**, *277*, 379.

(9) Kebarle, P.; Ho, Y. In *Electrospray Ionization Mass Spectrometry, Fundamentals, Instrumentation and Applications*; Cole, R. B., Ed.; John Wiley and Sons: New York, 1997; pp 3–64.

(10) Gieniec, J.; Fox, H. L.; Teer, D.; Dole, M. *Abstracts 20th ASMS Conf. Mass Spectrom. Allied Top.* 1972; 267.

(11) Dole, M.; Gupta, C. V.; Mack, L. L.; Nakamae, K. *Polym. Prepr., Am. Chem. Soc., Div. Polym. Chem.* **1977**, *18*, 188.

(12) Shumate, C. B.; Hill, H. H., Jr. *Anal. Chem.* **1989**, *61*, 601–606.

(13) Wittmer, D. H.; Chen, Y. H.; Luckenbill, B. K.; Hill, H. H., Jr. *Anal. Chem.* **1994**, *66*, 2348.

(14) Constantopoulos, T. L.; Jackson, G. S.; Enke, C. G. *Anal. Chim. Acta* **2000**, *406*, 37–52.

(15) Dole, M.; Mack, L. L.; Hines, R. L.; Mobley, R. C.; Ferguson, L. D.; Alice, M. B. *J. Chem. Phys.* **1968**, *49*, 2240–2249.

* To whom correspondence should be submitted. Phone: (509) 335-5648. Fax: (509) 335-8867. E-mail: hhhill@wsu.edu.

(1) Marquet, P.; Lacassie, E.; Battu, C.; Faubert, H.; Lachatre, G. *J. Chromatogr. B* **1998**, *700*, 77–82.

(2) Segura, J.; Ventura, R.; Jurado, C. *J. Chromatogr. B* **1998**, *713*, 61–90.

and Thomson¹⁶). Both models agree that the migration of positive ions (in positive mode) to the capillary/ESI needle tip incurs Coulombic forces between the ions to form a cone (Taylor cone).¹⁷ Because of instability created by repulsive forces between the ions, fine solution droplets are emitted from the cone. The two methods differ in their description of ion formation; the Dole charge residue model describes the ions forming infinitely smaller droplets until there is only one solute per droplet and the IEM states that as the solvent evaporates and concentrates the ions, the Coulombic repulsion forces become stronger than the analyte solvation energy, and ions are evaporated from the surface of the droplet in order to reduce the energy of the system.

Despite the proposed models and high volume of research involving ESI, several discrepancies still remain between the models and experimental observations.¹³ First, the relative intensities for many singly and doubly charged ions do not reflect the solution concentrations.¹⁸ This problem is extended when two or more analytes are present in solution, often resulting in preferential ionization of one or more species.¹³ Tang and Kebarle derived equations based on the IEM to describe the ionization efficiency for one analyte in a droplet¹⁹ and then to further describe the preferential ionization for two analytes.²⁰ Experimental data from Tang and Kebarle was fit to these equations for a one-analyte system.¹³ A second model (equilibrium partitioning model), which expanded on the ion evaporation model, was curve-fit to both one- and two-analyte systems with good experimental fits;¹⁸ however, there has been little additional research performed to determine solution parameters that may alter or improve the selective ionization of analytes.

The objectives of this study were to evaluate ESI-IMS/MS as a possible separation technique for amphetamine analysis. Figures of merit (limit of detection and limit of quantification) were evaluated for each compound. On the basis of the evaluation of amphetamines at high solution concentrations, preferential ionization of some amphetamines was found to occur. Charge competition processes among the six amphetamines were investigated, and the effect of solvent composition was studied. The data for one- and two-analyte systems were fit to the IEM models, and the solution composition results were explained on the basis of the IEM.

EXPERIMENTAL SECTION

Reagents. All electrospray solvents (methanol, water, and acetic acid) were obtained from J. T. Baker (Phillipsburg, NJ). The six amphetamine derivatives, (amphetamine (A), methamphetamine (MA), ethylamphetamine (EA), 3,4-methylenedioxymphetamine (MDA), 3,4-methylenedioxymethamphetamine (MDMA), and 3,4-methylenedioxyethylamphetamine (MDEA)) were purchased from Radian (Austin, TX) as 1 $\mu\text{g/mL}$ standards in methanol. Unless otherwise specified, the electrospray solvent composition was 47.5%/47.5% water/methanol with 5% acetic acid.

Instrumentation. The instrument consisted of 3 parts: an ESI source, an IMS, and a quadrupole mass spectrometer. The ESI is a water-cooled system that was developed at Washington State

University.¹³ A Brownlee Labs (Santa Clara, CA) dual-piston syringe pump was employed for solvent delivery. The electrospray flow rate was maintained at 5 $\mu\text{L/min}$. Injections were performed using a six-port (Valco Industries, Houston, TX) injection valve and a 70- μL external injection loop. For all experiments, 14 kV was applied to the electrospray needle, resulting in a +4 kV difference between the ESI needle and the target screen (first ring in the IMS drift tube).

The IMS system was built in-house at Washington State University. The basic design has been described previously⁴ and modifications to the original design were reported.¹⁹ The IMS was divided into two regions, the desolvation region (7.2 cm in length) and the drift region (22.5 cm in length), which were separated by a Bradbury–Nielsen-style ion gate. Both regions consisted of alternating alumina spacers and stainless steel rings with high-temperature resistors connecting the stainless steel rings (500 k Ω for the desolvation region, 1 M Ω for the drift region). Nitrogen was employed as both the drift gas and electrospray cooling gas (flow rates of 800 \pm 10 mL/min and 80 mL/min, respectively). The temperature in both the drift region and the desolvation region was maintained at 250 $^{\circ}\text{C}$ (\pm 10 $^{\circ}\text{C}$). Atmospheric pressure ranged from 690 to 705 Torr in Pullman, WA.

The IMS was interfaced to a model 150-QC ABB Extrel (Pittsburgh, PA) quadrupole MS via a 40- μm pinhole interface. The MS system has a m/z range of 0–4000 amu. Voltages on the transmitting lenses in the MS system were in the following order: +8.0 (pinhole), –12.6, –27.3, –14.6, –126.7, and –31.2 V. The polebias was operated at –15.2 V, and the dynode and the electron multiplier were set on 5 kV and –1.7 kV, respectively.

The output signal from the multiplier was connected to a Keithley model 427 amplifier (Keithley Instruments, Cleveland, OH) instead of the preamp originally configured for the MS. The amplified signal was then sent to either the MS data system or IMS system. A Merlin software system (ABB Extrel, Pittsburgh, PA) was utilized for all mass spectral analysis and mass spectrometer control. For the IMS gating and data acquisition, the electronic controls were built at Washington State University and have been described previously.¹³ The data acquisition and IMS gate-control software employed was Labview-based (National Instruments, Austin, TX) and modified at Washington State University.

In IMS, the separation occurs in milliseconds, and the complete separation is labeled as one IMS spectrum. Because of the reduction in ion population associated with the IMS/MS interface, it is common to average many single IMS spectra together to achieve a representative description of the ion population. The result of multiple averaged spectra is the IMS spectra reported in the figures presented in the Results section. In IMS, the separation time (or scan time) is determined by the time it takes the ion with the longest IMS transit time to travel through the drift tube. For example, small compounds, such as the amphetamines, typically have drift times of less than 25 ms, but larger ions, such as peptides, have drift times closer to 50 ms (these values are based on our current instrumental apparatus and drift gas). In this example, the scan or separation time for one mobility spectrum would be 25 ms for the amphetamines and 50 ms for the peptides.

(16) Iribarne, J. V.; Thomson, B. A. *J. Chem. Phys.* **1979**, *71*, 4451–4463.

(17) Taylor, G. I. *Proc. R. Soc. London A* **1964**, *A280*, 383.

(18) Enke, C. G. *Anal. Chem.* **1997**, *69*, 4885.

(19) Asbury, G. R.; Hill, H. H., Jr. *J. Microcolumn Sep.* **2000**, *12*, 391.

(20) Sunner, J.; Nicol, G.; Kebarle, P. *Anal. Chem.* **1989**, *60*, 1301–1307.

For each IMS spectra shown, 1000 single IMS spectra were averaged, and a scan time of 50 ms was used. As a result of additional processing overhead incurred by Labview (40%), complete acquisition of one spectra was performed in 70 s, although this analysis time could be reduced by optimizing the amount of averages and optimizing the scan time for each separation. For the separation of the six amphetamines, the longest drift time was less than 25ms. The scan time could be reduced to 25ms and allow for an analysis time of 35s.

Ion mobility spectra were obtained in two ways: nonmass-selective ion monitoring (NSIM) or mass-selective ion monitoring (SIM). In the first case, the IMS is continually gated and the MS is operated in the rf only mode with the DC voltage turned off. In the SIM mode, the quadrupole was operated with the DC voltage on to allow ions with a specific m/z to pass through the MS. The calibration curves and charge competition curves were obtained by setting the MS in the NSIM mode and transmitting all ions greater than or equal to a m/z of 136 (the m/z value for amphetamine, the smallest compound studied).

Figures of Merit. The limit of quantitation (LOQ) and limit of detection (LOD) for each amphetamine were calculated to be 10 and 3 times the signal-to-noise ratio, respectively. The LOQ and LOD were estimated from the analytical linear expressions obtained from the linear portions of the single-analyte calibration curves. Six concentrations (from 0.25 to 100 ppm) were analyzed for each calibration curve, and the average of three replicates was indicated by the points in Figure 3. Linearity for each curve was determined on the basis of a minimum r^2 value of 0.99.

Calculations. Reduced mobility values (K_0) values were calculated on the basis of the following equation,⁴

$$K_0 = \frac{f}{Vt_d} \frac{P}{760} \frac{273}{T} \quad (1)$$

where l is the length of the drift region (22.5 cm), V is the voltage applied to the drift region (8.3kV), t_d is the drift time (ms), P is the atmospheric pressure (690–705 Torr), and T is the temperature of the drift region (250 °C).

On the basis of IEM theory,²² the following equation describes the ion evaporation rate for an analyte (A) in comparison to the evaporation rate of the solution electrolyte (E):

$$I_{(A^{+},g)} = pf \left(\frac{k_A[A^+]}{k_E[E^+] + k_A[A^+]} \right) I \quad (2)$$

where $I_{(A^{+},g)}$ is the gas-phase analyte ion current, k_A and k_E are rate constants that express the rate of ion transfer from the droplets to the gas phase for the analyte and electrolyte, respectively, $[A^+]$ and $[E^+]$ are the analyte and electrolyte solution concentrations, f is the fraction of droplet charge that gets converted into the gas phase, p is the transmission efficiency of ions through the ion mobility spectrometer and mass spectrometer, and I is the total ion current. The measured gas-phase analyte ion current was adjusted for the mass-dependent transmission

Table 1. Reduced Mobility Values (K_0) and Literature K_0 Values for Six Amphetamines Employed in This Study^a

amphetamine	MW (amu)	drift time (ms)	K_0 (cm ² V ⁻¹ s ⁻¹)	lit. K_0 (cm ² V ⁻¹ s ⁻¹)
AM	135	18.50	1.62	1.66 (25)
MA	149	18.85	1.59	1.63 (25)
EA	163	19.60	1.53	
MDA	179	20.65	1.45	1.49 (25)
MDMA	193	21.05	1.42	1.4733 (5)
MDEA	207	21.75	1.37	1.4201 (5)

^a All reference values were obtained with air as the drift gas. Parentheses contain the reference number.

Table 2. Linear Regression Data, Limit of Detection, and Limit of Quantitation for Six Amphetamines^a

amphetamine	slope	y-intercept	R^2	LOD ppb (pmol)	LOQ ppb (pmol)
AM	0.0602 ^b	0.0004	0.9933	42.3 (1.35)	141 (4.52)
MA	0.0834 ^b	-0.0557	0.9902	20.8 (0.604)	69.3 (2.01)
EA	0.0270 ^c	0.0957	0.9897	15.4 (0.408)	51.3 (1.36)
MDA	0.0299 ^c	0.0180	0.9904	71.8 (1.73)	239 (5.78)
MDMA	0.0402 ^c	0.0401	0.9977	32.4 (0.727)	108 (2.42)
MDEA	0.0610 ^c	-0.0057	0.9984	22.8 (0.478)	76.0 (1.59)

^a Reported values in pmol for LOD/LOQ are based on an ESI flow rate of 5 μ L/min and a 52-s analysis time. ^b Linear over 3 orders of magnitude. ^c Linear over 3.5 orders of magnitude.

Table 3. Relative Mass-Dependent Transmission Efficiencies,^a Ion Evaporation Rate Constants,^b the Normalized k_A Values, and the R^2 Values for the Curve Fits to Eq 2

amphetamine	T_m^c	k_A^d	normalized k_A	R^2
AM	1.000	0.310	1.00	0.851
MA	0.962	0.782	2.52	0.984
EA	0.925	0.435	1.40	0.994
MDA	0.882	0.546	1.76	0.995
MDMA	0.844	0.927	2.99	0.997
MDEA	0.807	1.267	4.08	0.999

^a T_m ^b Determined according to eq 2. ^c T_m values were calculated on the basis of data from ref 20 and were normalized on the basis of a transmission efficiency of 1.00 for amphetamine. ^d The k_A values were calculated from the curve fits by setting k_E equal to 1.00 where values <1.00 indicated lower rate constants than the electrolyte. ^e The normalized k_A values were relative to the k_A value for amphetamine. A value >1.00 indicated a greater evaporation rate than amphetamine

(T_m) by dividing the measured analyte intensity by the T_m to obtain the $I_{(A^{+},g)}$ for each compound.²⁰ The T_m values for the ABB quadrupole mass spectrometer were obtained from the company according to the instrumental specifications.²¹ The T_m values are shown in Table 3. Similarly to previous studies, the f value was assumed to be 0.3 (~30% conversion of charge from the droplet to the gas phase). The p value due to both the IMS and MS transmission efficiency (based on 0.2-ms pulse width, 50-ms scan time, and 40- μ m-diameter pinhole interface) was determined to be $\sim 4 \times 10^{-9}$ and was similar to the values obtained in previous

(21) Pedder, R. E.; Schaeffer, R. A. ABB Extrel Internal Document; Note RA_2001B.

(22) Kebarle, P.; Tang, L. *Anal. Chem.* **1993**, *65*, 972A.

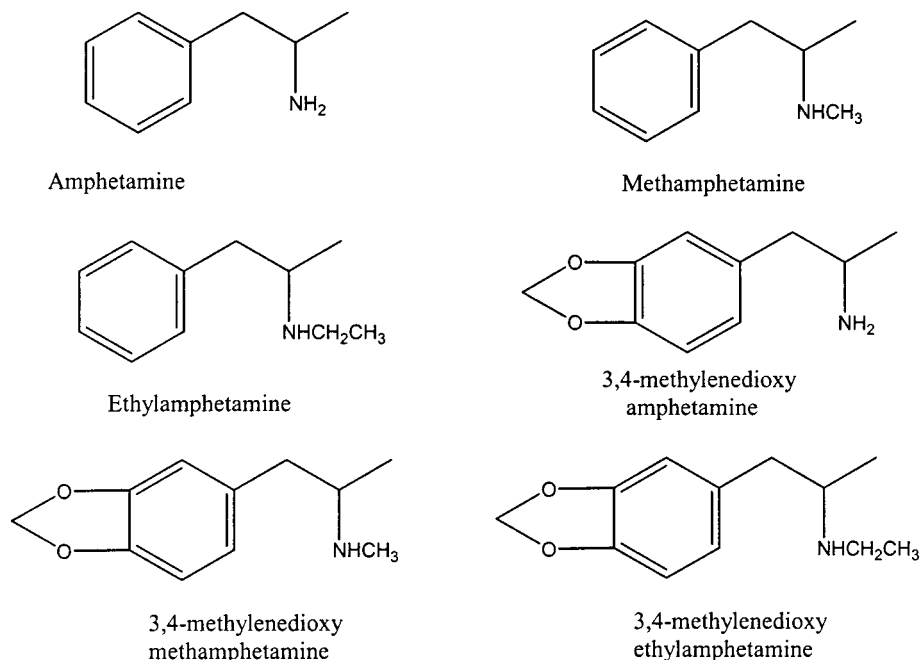


Figure 1. Molecular structures for the 6 amphetamines that were studied.

studies ($\sim 10^{-6}$ transfer efficiency in the MS due to the interface).²² The rate constants were normalized on the basis of a k_E for the electrolyte of 1.0.

For two analytes, the following equation was employed to describe the relative evaporation rates,

$$I_{(A^+,g)} = pf \left(\frac{k_A[A^+]}{k_E[E^+] + k_B[B^+] + k_A[A^+]} \right) I \quad (3)$$

where k_B is the ion evaporation rate constant for the second analyte (B) and $[B^+]$ was the solution concentration.

RESULTS AND DISCUSSION

Amphetamine Separation by ESI-IMS/MS. Six amphetamines were evaluated in this study: AM, MA, EA, MDA, MDMA, and MDEA. With the exception of EA, the amphetamines are abused drugs or metabolites of the drugs and were chosen for their analytical relevance. Molecular structures for each of the drugs are shown in Figure 1. The compounds are divided into two classes: simple amphetamines (AM, MA, and EA) and 3,4-methylenedioxyamphetamine derivatives (MDA, MDMA, and MDEA). Each class contains one compound with a proton on the amine (AM and MDA), a methyl group on the amine (MA and MDMA), and an ethyl group on the amine (EA and MDEA).

Figure 2 shows the separation of the six amphetamines by ESI-IMS/MS. Figure 2a shows the nonselective IMS spectra of the mixture and Figure 2b shows each mass-identified IMS mobility peak. Each ion was mass-identified to be the protonated molecular ion, and these results were similar to ions observed previously in ESI and secondary-ESI.⁶ When compared to traditional chromatographic analysis times, the analysis time of 70 s was at least 1 order of magnitude better. In addition, the instrument's downtime between runs was minimized in comparison with chromatographic techniques that must reduce temperature or flush the mobile phase prior to a new run.

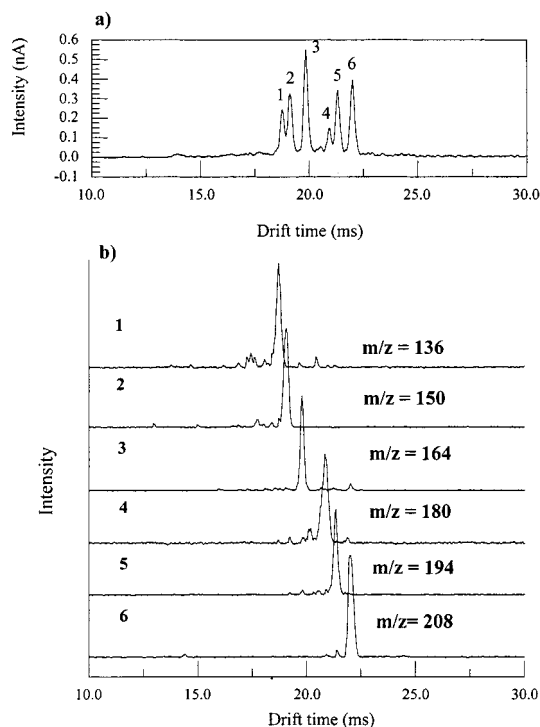


Figure 2. ESI-IMS/MS spectrum of amphetamine mixture: (a) nonselective IMS spectrum (mass spectrometer excluded ions less than 130 m/z); (b) selective ion monitoring IMS spectrum (m/z value corresponds to MH^+ ion for each amphetamine). Amphetamines as follows: 1, amphetamine; 2, methamphetamine; 3, ethylamphetamine; 4, 3,4-methylenedioxyamphetamine; 5, 3,4-methylenedioxy methamphetamine; and 6, 3,4-methylenedioxyethylamphetamine.

As seen in Figure 2a, baseline separation was achieved for the amphetamines, except between AM/MA and MDA/MDMA. On the basis of the two-peak resolution definition employed in IMS,¹⁹

$$R = 2^* \left(\frac{t_{d2} - t_{d1}}{w_{b1} + w_{b2}} \right) \quad (4)$$

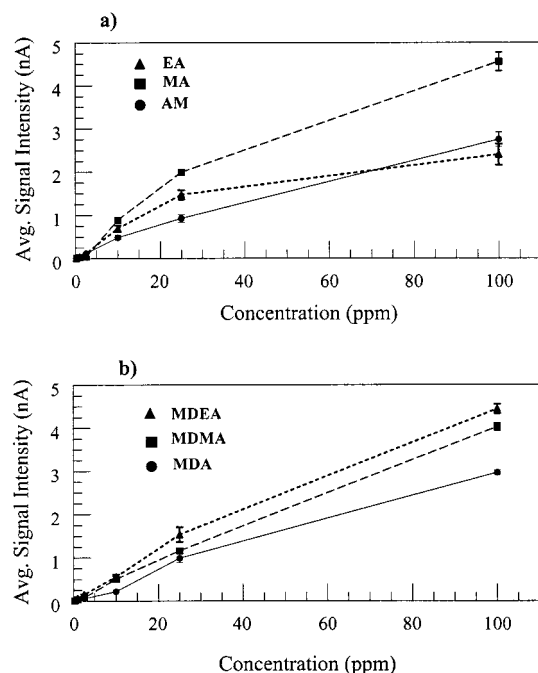


Figure 3. Calibration curves for six amphetamines over 4 orders of magnitude: (a) simple amphetamines and (b) methylene dioxy derivatives.

(where t_d is the drift time of the two consecutive peaks, w_b is the peak width at the base), the resolution for the two nonbaseline resolved pairs (AM/MA and MDA/MDMA) can be compared. For the first and second pair, the resolution was determined to be 0.8 and 1.0, respectively. On the basis of the common chromatographic resolution of 1.0 to indicate resolution, the MDA/MDMA pair was separated. Although the separation of AM and MA proved more difficult, two-dimensional information of the mobility and m/z identification allowed for confident determination of all six amphetamines. The K_0 values were calculated based on eq 1 and are presented in Table 1. Literature K_0 values are also listed in Table 1, although they were not directly comparable, because the reference values were obtained with air as the drift gas.⁵ On the basis of a comparison of K_0 values reported for different compounds in both air and nitrogen, the difference in K_0 units of $0.05 \text{ cm}^2 \text{ V}^{-1} \text{ s}^{-1}$ is consistent with a standard K_0 difference of 5%²³ (3% difference for AM).

Figures of Merit. For each amphetamine, figures of merit were determined. First, a calibration curve for each compound was acquired. Calibration curves for the two classes of amphetamines are shown in Figure 3a (simple amphetamines) and b (methylene dioxy derivatives). Several interesting features can be ascertained from Figure 3. First, there were two distinct regions observed for each curve, a linear portion and an upper limit. These two regions are similar to the results obtained in both ESI-MS^{9,18} and ESI-IMS.⁶ As seen in Figure 3, the upper intensity limits differed for the six compounds. The lowest currents were observed for AM and MDA, and the highest occurred for MA and MDEA. For all six compounds, the linear portions extended to at least 2.5 orders of magnitude. The r^2 value and slope for each calibration line were reported in Table 2. For all six compounds, the r^2 values

were greater than 0.99, indicating linearity within the concentrations studied.

In addition, LODs and LOQs are reported in Table 2. For the two classes, the ethylamphetamines had the lowest detection limits. The LODs were similar to values reported in GC/MS³, and ESI-IMS/MS obtains sensitivities similar to traditional chromatographic methods. The LODs ranged from 15.4 ppm (EA) to 71.8 ppm for MDA.

Single-Analyte Ion Evaporation Models. Early in these studies, preferential ionization between the amphetamines was observed. On the basis of these initial observations, the calibration curves shown in Figure 3 were fit to a rearranged form of eq 2 (the equation was divided by k_A in order to determine k_E/k_A). In the original work of Tang and Kebarle, the k_E values were assumed to be 1 in order to determine the k_A values.²² On the basis of this method, the calculated k_A values are reported in Table 3. These ion evaporation rates are relative to the evaporation rate of the electrolyte (protons) and provide a qualitative comparison between the electrolyte and the analytes. In a quadrupole MS, the transmission efficiency for an ion is known to be mass-dependent, and the measured analyte currents were corrected for the mass dependent transmission efficiency (T_m), also listed in Table 3. Along with these values, the normalized ion evaporation rates (relative to amphetamine) and the R^2 values for the curve fits were reported. The curve fit regressions were within 0.9 for all of the analytes except amphetamine.

An ion evaporation rate of less than 1 means that the analyte ions evaporate slower than the electrolyte. For the six amphetamines, only MDEA had a greater rate than the electrolyte. In general, the evaporation rates increased in the following trends; proton < methyl < ethyl and simple amphetamines < methylenedioxyamphetamines. However, the rate for MA was greater than the rate for EA. This relation between MA and EA was also reflected in the upper intensity limits shown in Figure 3 but not reflected in the detection limits. The normalized k_A values showed that the greatest ion evaporation rate was obtained for MDEA, and the lowest was found for AM.

Ion evaporation rates provide a qualitative description of the rate at which ions are emitted from the ESI droplets into the gas phase. Greater evaporation rates would lead to an increase in the number of ions in the gas phase and would be measured as an increase in the analyte ion intensity. Therefore, the evaporation rates would be expected to predict the preferential ionization of analytes and their relative intensities when present as a mixture.

In Figure 4a, a typical solvent IMS spectra is shown. The ions between 10 and 15 ms were solvent ions, and their identities have been discussed previously.⁴ In Figure 4b, a mixture of the six amphetamines (10 ppm each) was analyzed. Because of the addition of the amphetamines, the solvent ions were reduced in intensity, and all six ions were easily identified. Although all six amphetamines were observed, the relative signal intensities were different. With the exception of EA, the relative intensities were predicted by the evaporation rates. For example, AM responded the least strongly in Figure 4b, and it had the smallest k_A value (0.310) (see Table 2). Comparison among the relative intensities of MDA, MDMA, and MDEA and the ion evaporation rates showed similar trends. Except for EA, the relative ionization

(23) Shumate, C.; St. Louis, R. H.; Hill, H. H., Jr. *J. Chromatogr.* **1986**, *373*, 141–173.

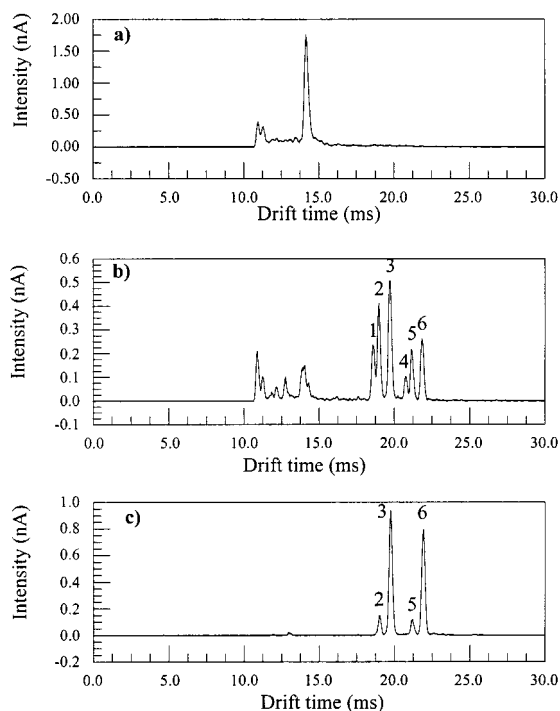


Figure 4. Nonselective ESI-IMS/MS spectrum of amphetamine mixture and solvent. The ESI solvent was 47.5% water/47.5% methanol with (b) mixture of 6 amphetamines at 10 ppm each, (c) mixture of 6 amphetamines at 100 ppm each. Graph shows charge competition between amphetamine compounds. Amphetamines as follows: 1, amphetamine; 2, methamphetamine, 3, ethylamphetamine; 4, 3,4-methylenedioxyamphetamine; 5, 3,4-methylenedioxy methamphetamine; and 6, 3,4-methylenedioxyethylamphetamine. 5% acetic acid. (A) ESI solvent spectrum.

efficiencies for a similar series of molecules were predictable simply on the basis of the calibration curve and curve fits to eq 2.

Because of the difference in ionization efficiencies at 10 ppm, the mixture was also evaluated at 100 ppm (Figure 4c). At the higher concentrations, the solvent ions were not observed in the IMS spectra, an indication that the maximum amount of charge had been utilized for ionization of the amphetamines. Increasing the concentration by a factor of 10 to 100 ppm for each amphetamine resulted in only four of the six amphetamines being observed. Even though each amphetamine was present at equal concentrations, charge competition within the ESI droplets reduced the response of the amphetamines (AM and MDA) and also slightly reduced the signal intensity of the methamphetamine compounds (MA and MDMA).

Several trends in the ESI ionization efficiency for amphetamines were demonstrated in Figure 4. First, the ethylamphetamines responded strongest within each class, and the functional group (proton, methyl, ethyl) correlated with increasing ionization efficiency of the molecule for both amphetamine classes. Referring back to Figure 1, the amphetamine structures show that the more nonpolar the functional group, the greater the calculated evaporation rate. These results were similar to a recent study by Enke et al. that compared the polarity of amino acids to the ESI ionization efficiency and found that nonpolar amino acids provided the greatest responses.²⁴

Two-Analyte Ion Evaporation Models. On the basis of the evidence of selective ionization between the amphetamines, further investigation into the analyte competition was performed. In addition, modifications in ESI solution composition to improve the ionization efficiency of the analytes were studied. Charge competition within the ESI process has been observed for many years and has been a major limitation for ESI-MS of complex mixtures. Because of the complexity of ESI and the discrepancy in mechanistic models, predictions of parameters that may reduce preferential ionization have been difficult and limited. The models that have been used to describe the charge competition phenomena employ the analyte(s) concentration and electrolyte concentration, as described in eq 2 and 3. For cases in which experimental data has been fit to the models, the electrolytes that were considered have simply been solvent impurities.²² Common ESI solvents typically contain a modifier that increases the ESI current and analyte sensitivity. For our instrument and ESI source, addition of 5% acetic acid has been found to increase analyte signal intensity and is commonly used as the optimal ESI solvent.⁶ The effect of common modifiers on charge competition was investigated for two and three analyte systems. The underlying question was what effect the electrolyte had on preferential ionization of the amphetamines. Because of the similar trends in behavior of the simple and methylene dioxy amphetamines, only the simple amphetamines were evaluated. Calibration curves for 2-analyte mixtures (AM and MA) and 3-analyte mixtures (AM, MA, and EA) were obtained.

The calibration curves for the two-analyte systems are shown in Figure 5: (a) 5% acetic acid, (b) 1% formic acid, and (c) 50/50 water/methanol. In part a, the solvent conditions were the same as those for the single analyte calibration curves, and any differences were a result of the two analytes. Until 100 ppm, the response for both analytes was similar to the single analyte curves. Both were linear from 25 ppm with excellent R^2 values (see Table 4). In contrast to the single analyte curves, the AM response decreased to below the detectable limit at 100 ppm. These results indicated that the charge competition between the two analytes increased the MA signal and significantly reduced the AM signal.

All concentrations and parameters in Figure 5a–c, were the same except the solvent composition. In all three cases, the bulk solution was composed of 50% water and 50% methanol, and in parts a and b, modifiers were added. Therefore, differences in the three graphs were due to the modifiers. In Figure 5b, (1% formic acid), the trends in charge competition between AM and MA were similar to part a, although the magnitude was different. First, the AM response was linear only for 2.5 orders of magnitude, but MA was still linear to 3. Furthermore, the difference in responses between AM and MA was greater in part b (2 and 8 nA) than in part a (4 and 7 nA, respectively) at a concentration of 25 ppm each. For the two-analyte system, the addition of 1% formic acid increased the degree of charge competition.

In Figure 5c, the solvent was sprayed without the addition of a modifier, and this was found to reduce the amount of charge competition. Even when both analytes were present at concentrations of 100 ppm, the AM signal was observed. In addition, up to 10 ppm, the signal intensities for AM and MA were very similar. On the basis of these results, it appeared that the lack of modifier

(24) Cech, N. B.; Enke, C. G. *Anal. Chem.* **2000**, *72*, 2717–2723.

(25) Lawrence, A. H. *Anal. Chem.* **1988**, *58*, 1269–1272.

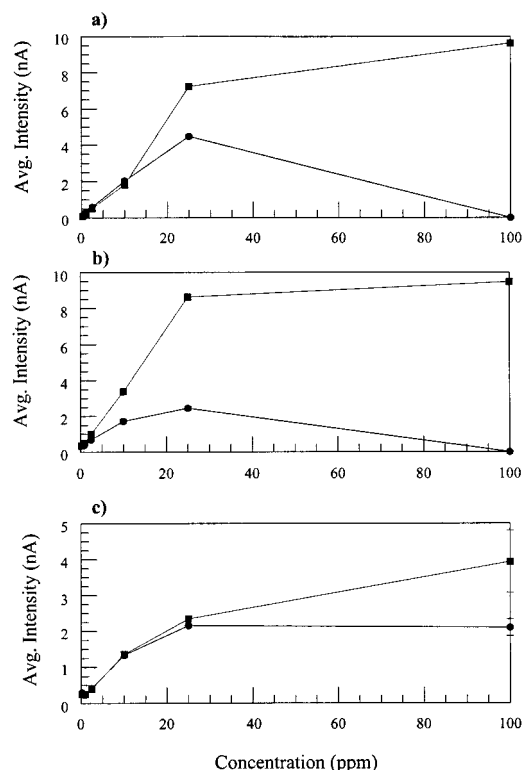


Figure 5. Two-analyte calibration curves with different solvent modifiers: (a) 5% acetic acid, (b) 1% formic acid, and (c) without modifier. All solvents were made with 50% water/50% methanol. Six calibration points were obtained for each compound, and the concentration of the three compounds was equal where $[AM] = [MA]$. ■, MA; and ●, AM.

Table 4. Data Generated from Two-Analyte Calibration Curves^a

	50% water	1% formic acid	5% acetic acid
K_{AM}/k_{MA}	1.60	0.168	0.0547
k_E/k_{MA}	.512	0.131	0.221
R^2	0.995	0.951	0.951
AM slope	0.125 ^b	0.336 ^c	0.292 ^c
AM R^2 value	0.999	0.999	0.999
MA slope	0.114 ^b	0.143 ^b	0.176 ^c
MA R^2 value	0.983	0.998	0.998

^a Top constants generated from curve fits of eq 3 to the curves. Bottom slopes and linear regression values for two-analyte calibration curves in three different solvent compositions. ^b Linear over 2.5 orders of magnitude. ^c Linear over 3.0 orders of magnitude.

reduced the charge competition and allowed an AM response to be observed, even at high concentrations.

In Table 4 (bottom), the slopes and r^2 values were reported for AM and MA in each of the three solvent compositions. It is important to note some general trends in the compound linearity and intensities observed with the three solvent compositions. The slopes were different for each analyte in each solvent composition. A larger slope indicated a greater sensitivity for that analyte. On the basis of the slopes, the greatest sensitivity for AM was observed in 5% acetic acid and for MA, was observed in 1% formic acid. Although the 50/50 water/methanol solvent reduced charge competition, it also provided the lowest sensitivities for both compounds. On the basis of these studies, there appeared to be

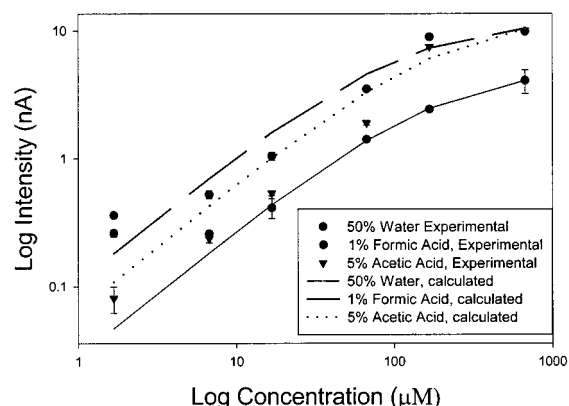


Figure 6. Experimental and calculated curve-fit data for methamphetamine at three different solvent compositions. Experimental data points for three solvent conditions were curve-fit to eq 3, and the curve fits are represented as the lines on the figure. Graph shows how well the two-analyte ion evaporation model correlated with the experimental points.

a tradeoff between the optimal conditions for analyte sensitivity and reduction in analyte charge competition.

To determine mechanistic relationships for the three ESI solvent conditions, the two-analyte curves were fit to eq 3 (where MA was A, and AM was B). The ion evaporation rates for AM and MA and the R^2 values for the curve fits are reported in Table 4. For both 1% formic acid and 5% acetic acid, the R^2 values were ~ 0.95 and were not as good as for the single analyte curves. However, some qualitative relationships can be drawn from the curve fits. First, the k_{AM}/k_{MA} values were the lowest for the 5% acetic acid (0.0547) and the greatest for the 50/50 water/methanol solution (1.60). A k_{AM}/k_{MA} of <1.0 indicates that the ion evaporation rate for AM is less than that of MA. In both 5% acetic acid and 1% formic acid, the k_{AM} was less than that of MA. Comparison with the curves in Figure 5 shows that this relationship is supported by the disparity in AM intensity at the higher concentrations. Interestingly, the 50/50 water/methanol solution provided similar AM and MA intensity values and this is supported by the relative rates reported in Table 4.

The rates showed that the 50/50 water/methanol solution provided both relative evaporation rates for AM and MA. Inspection of the k_E/k_{MA} values showed that there was a similar increase in value from 0.131 (1% formic acid) to 0.512 (50/50 water/methanol). This indicated that the MA evaporation rate approached that of the electrolyte with the removal of the modifiers from the ESI solution. Since the mechanistic model used in these analysis provided only relative comparison, it is difficult to identify the exact chemistry that occurred within the ESI droplet; however, the ESI solution and modifiers changed both the relative rates between MA and AM and MA and the electrolyte. The modifiers increased the overall analyte current and the evaporation rates in comparison to the electrolyte.

In Figure 6, the curve fits for the three solution compositions are shown, along with the experimental data points. It appeared that the calculated curve fits approached the data points at higher concentrations, and greater deviations were seen at the lower analyte concentrations; however, the equations did predict the upper intensity limits quite accurately.

Charge Competition within Three-Analyte System. The addition of a third analyte (EA) provided a more complex system

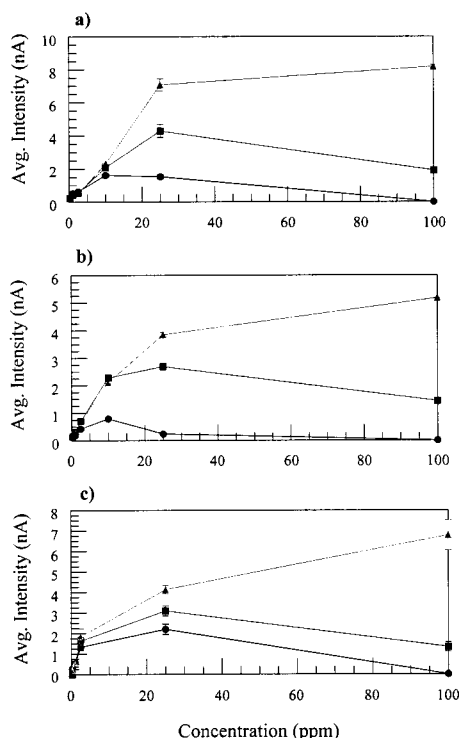


Figure 7. Three-analyte calibration curves with different solvent modifiers: (a) 5% acetic acid, (b) 1% formic acid, and (c) without modifier. All solvents were made with 50% water/50% methanol. Six calibration points were obtained for each compound, and the concentration of the three compounds was equal where $[AM] = [MA] = [EA]$. Symbols: \blacktriangle , EA; \blacksquare , MA; and \bullet , AM.

to be investigated and then compared with the two-analyte system. The same three solvent compositions as shown in Figure 5 were evaluated and are shown in Figure 7. The only difference between Figures 5 and 7 was the addition of a third analyte (EA). Both 5% acetic acid (a) and 1% formic acid (b) provided the highest degree of charge competition, with EA being the predominant ion at higher concentrations and AM being the lowest responding analyte. Although the addition of EA reduced the intensity of MA, a response was still observable at very high concentrations. Similar to the results in Figure 5, 50/50 water/methanol (c) was found to provide the least degree of charge competition. However, AM was still not observed at 100 ppm, even in part c. The data in

Figure 7 was curve-fit to a three-analyte equation (similar to eq 3), but significant deviations were observed.

CONCLUSIONS

The separation of six amphetamines by ESI-IMS/MS was shown and found to be a sensitive and rapid analytical method for amphetamine analysis. In reality, the analysis of biological samples by ESI-IMS/MS would probably have to be preceded by an extraction step. Combining an extraction step with the use of an internal standard would enable ESI-IMS/MS to be utilized as a separation tool for the amphetamines. Further research is required with biological samples in order to completely determine the capabilities of ESI-IMS/MS; however, the speed of separation and sensitivity make the technique attractive as an alternative to chromatographic methods.

In addition, solutions to charge-competitive processes were discussed. The optimal ESI conditions for analyte sensitivity (5% acetic acid modifier) were found to increase selective ionization between the amphetamines. The removal of modifiers from the ESI solution was found to improve the degree of charge competition and enabled all three amphetamines to be observed.

On the basis of the curve fits to the ion evaporation model equations, increases in ion evaporation rates for some analytes (MA) were found to occur with the addition of modifiers. This would be expected, because these volatile modifiers are frequently employed to improve sensitivity; however, it appeared that the modifiers were selective at high concentrations to improve sensitivity for certain analytes but not others. A greater understanding of the solution and ion chemistry governing the ESI process would provide information about why the solution parameters alter the evaporation rates. This is the first study in which the solution compositions have been investigated in order to understand the selective ionization processes.

ACKNOWLEDGMENT

This work was supported by the National Institutes of Health (Grant 8RO3DA1192302) and the National Science Funding (Grant CHE9870850). The authors thank the National Institutes of Drug Abuse for the scholarship funding for L. M. Matz.

Received for review July 31, 2001. Accepted October 25, 2001.

AC010858M